

Controlling Defect-State Photophysics in Covalently Functionalized Single-Walled Carbon Nanotubes

Brendan J. Gifford, Svetlana Kilina, Han Htoon, Stephen K. Doorn,* and Sergei Tretiak*



Cite This: *Acc. Chem. Res.* 2020, 53, 1791–1801



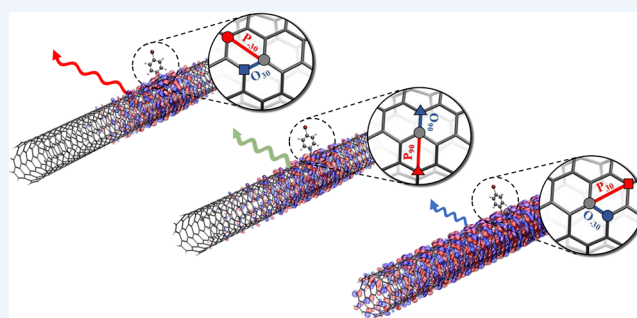
Read Online

ACCESS |

Metrics & More

Article Recommendations

CONSPECTUS: Single-walled carbon nanotubes (SWCNTs) show promise as light sources for modern fiber optical communications due to their emission wavelengths tunable via chirality and diameter dependency. However, the emission quantum yields are relatively low owing to the existence of low-lying dark electronic states and fast excitonic diffusion leading to carrier quenching at defects. Covalent functionalization of SWCNTs addresses this problem by brightening their infrared emission. Namely, introduction of sp^3 -hybridized defects makes the lowest energy transitions optically active for some defect geometries and enables further control of their optical properties. Such functionalized SWCNTs are currently the only material



exhibiting room-temperature single photon emission at telecom relevant infrared wavelengths. While this fluorescence is strong and has the right wavelength, functionalization introduces a variety of emission peaks resulting in spectrally broad inhomogeneous photoluminescence that prohibits the use of SWCNTs in practical applications. Consequently, there is a strong need to control the emission diversity in order to render these materials useful for applications. Recent experimental and computational work has attributed the emissive diversity to the presence of multiple localized defect geometries each resulting in distinct emission energy. This Account outlines methods by which the morphology of the defect in functionalized SWCNTs can be controlled to reduce emissive diversity and to tune the fluorescence wavelengths. The chirality-dependent trends of emission energies with respect to individual defect morphologies are explored. It is demonstrated that defect geometries originating from functionalization of SWCNT carbon atoms along bonds with strong π -orbital mismatch are favorable. Furthermore, the effect of controlling the defect itself through use of different chemical groups is also discussed. Such tunability is enabled due to the formation of specific defect geometries in close proximity to other existing defects. This takes advantage of the changes in π -orbital mismatch enforced by existing defects and the resulting changes in reactivities toward formation of specific defect morphologies. Furthermore, the trends in emissive energies are highly dependent on the value of $\text{mod}(n-m,3)$ for an (n,m) tube chirality. These powerful concepts allow for a targeted formation of defects that emit at desired energies based on SWCNT single chirality enriched samples. Finally, the impact of functionalization with specific types of defects that enforce certain defect geometries due to steric constraints in bond lengths and angles to the SWCNT are discussed. We further relate to a similar effect that is present in systems where high density of surface defects is formed due to high reactant concentration. The outlined strategies suggested by simulations are instrumental in guiding experimental efforts toward the generation of functionalized SWCNTs with tunable emission energies.

KEY REFERENCES

- Gifford, B. J.; Kilina, S.; Htoon, H.; Doorn, S. K.; Tretiak, S. Exciton Localization and Optical Emission in Aryl-Functionalized Carbon Nanotubes. *J. Phys. Chem. C* **2018**, 122 (3), 1828–1838.¹ *This theoretical investigation demonstrated the impact of defect geometry on electron and exciton localization and the resulting impact on electronic states and optical transition energies. This suggests that spectral diversity in functionalized SWCNT samples can be attributed to the existence of distinct defect morphologies.*
- Saha, A.; Gifford, B. J.; He, X.; Ao, G.; Zheng, M.; Kataura, H.; Htoon, H.; Kilina, S.; Tretiak, S.; Doorn, S.

K. Narrow-Band Single-Photon Emission through Selective Aryl Functionalization of Zigzag Carbon Nanotubes. *Nat. Chem.* **2018**, 10 (11), 1089.² *This report computationally and experimentally explains the impact of SWCNT chirality on the optical transition and*

Received: April 15, 2020

Published: August 17, 2020



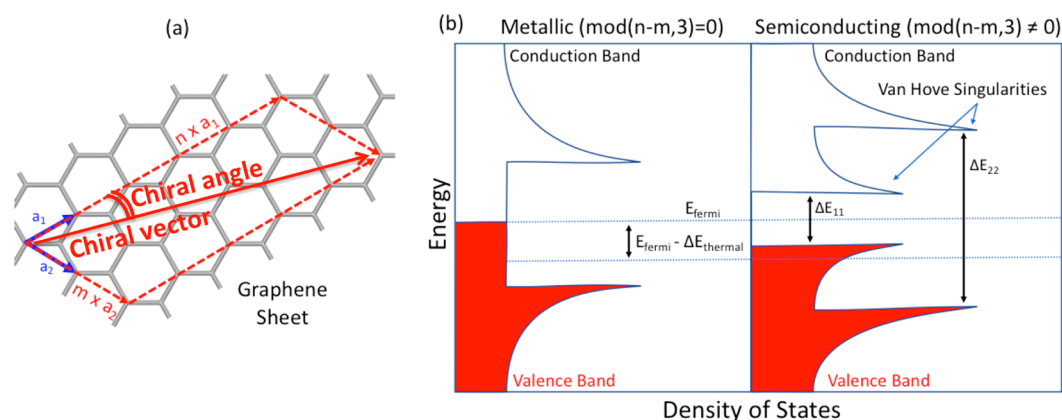


Figure 1. (a) Graphene sheet that is rolled into a cylinder following the chiral angle to form a SWCNT. The vectors a_1 and a_2 represent the unit vectors of the graphene lattice that determine SWCNT geometry and (b) the resulting electronic structure of a SWCNT. Reproduced with permission from ref 43. Copyright 2019 American Chemical Society.

spectral energies. Which defect geometries are formed in experimental samples are then demonstrated, and it is inferred that pi-orbital mismatch plays a strong role in the formation of some defect morphologies over others.

- Gifford, B. J.; He, X.; Kim, M.; Kwon, H.; Saha, A.; Sifain, A. E.; Wang, Y.; Htoon, H.; Kilina, S.; Doorn, S. K.; Tretiak, S. Optical Effects of Divalent Functionalization of Carbon Nanotubes. *Chem. Mater.* **2019**, *31* (17), 6950–6961.³ This report details the impacts of restricting the morphologies of defects that can form through divalent functionalization of several different classes as well as by controlling concentration. The impact of hybridization of the defected carbon atoms on spectral red-shifts are explained in detail.
- Gifford, B. J.; Saha, A.; Weight, B. M.; He, X.; Ao, G.; Zheng, M.; Htoon, H.; Kilina, S.; Doorn, S. K.; Tretiak, S. Mod(n-m,3) Dependence of Defect-State Emission Bands in Aryl-Functionalized Carbon Nanotubes. *Nano Lett.* **2019**, *19* (12), 8503–8509.⁴ This report details the energies of spectral features resulting from functionalization of SWCNTs of different mod(n-m,3) classes with similar defect morphologies. It further describes the physical source of stronger red-shifts from certain defect morphologies based on the ground state electronic structure of the functionalized species.

■ INTRODUCTION

Single-walled carbon nanotubes (SWCNTs) are constructed from a network of sp^2 hybridized carbon atoms assembled in a cylindrical form.^{5,6} The geometry of a SWCNT is uniquely defined by the “chirality”, i.e., two chiral indices n and m , determining a roll-up angle for folding a graphene sheet into the tube (Figure 1a).⁷ The chirality of the nanotube also determines its electronic⁸ (Figure 1b) and optical⁹ properties. Due to this tunability via geometrical parameters, a wide range of photoluminescence energies can be accessed,¹⁰ making SWCNTs promising for use in fiber optic applications¹¹ including secure communications and quantum computing.¹² For communications, light wavelengths of 1530–1565 nm are desired due to the transparency in transmission for materials in this range.¹¹ As such, there is a significant demand in developing single-photon sources that generate such light.^{13–15} SWCNTs are potentially able to produce desired

infrared emission features depending on the tube structure. However, their application is limited due to quenching from a rapid exciton diffusion and the presence of low-energy nonemissive states in SWCNTs.^{16,17} Furthermore, the SWCNTs required to achieve the target emissive wavelengths are relatively large in diameter.¹⁸ Difficulties in separation persist for this large size range due to a high diversity of chiralities that exists with similar diameters.^{19–22} The most common CoMoCat²³ and HiPCo²⁴ synthetic methods produce tubes of much smaller diameters than species required for this application. Postsynthetic chemical functionalization of pristine SWCNTs has been suggested as an alternative way to increase their practicality for fiber optical applications.^{25,26}

Covalent bonding of a functional group to the SWCNT surface generally creates an sp^3 -defect at the sp^2 -hybridized tube's lattice. Light absorption in SWCNT systems generally occurs on the pristine portion at the E_{22} band energies typically corresponding to the visible wavelength range and E_{11} band energies around 1000–1200 nm (Figure 1b), resulting in the generation of an exciton. The fast-moving exciton subsequently is trapped at the site of covalent functionalization,²⁷ resulting in a spatially localized exciton around the defect. The sp^3 -defect causes perturbations to the electronic structure of the functionalized system and results in smaller energy gaps at the defect site.^{28–30} This red-shifts photoluminescence to wavelengths by as much as 400 nm and moves functionalized small-diameter SWCNTs closer to the desired target frequency range for devices.¹¹ Furthermore, chemical functionalization brightens the lowest-energy transitions,¹⁷ thereby increasing the photoluminescence quantum yields by nearly an order of magnitude.²² Such functionalized SWCNTs are the first material to exhibit single-photon emission at telecom wavelengths and at room-temperature,^{26,17,31,32} generating a substantial interest into their synthesis and characterization. While these are desirable characteristics for the use in devices, chemical functionalization introduces several emission features of different energies in the near-infrared range.^{1,11,33} While the presence of multiple features can be used to tune the materials where specific energy ranges are desired, applications utilizing functionalized SWCNTs generally require homogeneous emission at a specific energy. As such, a great deal of recent research focuses on strategies toward precise control of their photoluminescence characteristics. Such strategies include controlling the functionalizing species,³⁴ localized defect

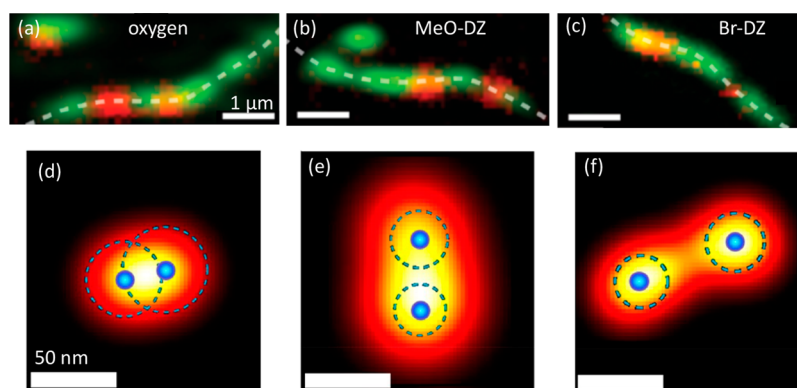


Figure 2. (a–c) Photoluminescence images of three individual (6,5) SWCNTs functionalized with oxygen, 4-methoxybenzenediazonium (MeO–DZ) and 4-bromobenzenediazonium (Br–Dz). While the band-edge PL emission is delocalized over the entire length of the SWCNT (5–6 μm) (green), the defect PL emission (red) is observed to localized to diffraction limited spots.²³ (d–f) Super-resolution photoluminescence images of ultrashort (<50 nm) SWCNT functionalized with perfluorinated hexyl chains at the end of the SWCNTs demonstrate that sp^3 defects created at the end emit PL localized to <25 nm (resolution limit) from the ends. Ultrashort SWCNT without functionalization cannot emit PL due to strong nonradiative PL quenching at the ends.⁴⁰ These studies provide clear evidence on localization of the excitons to a potential well around the sp^3 defects. Figures adapted with permission from refs 27 and 39. Copyright 2015 Royal Society of Chemistry and 2018 American Chemical Society.

geometry,^{1,3,35} SWCNT chirality,^{2,4} and defect concentration.³ By emphasizing joint modeling and experimental insights, this Account focuses on how these characteristics of the sp^3 defect in functionalized SWCNTs affect the energies of the optical emissive features and how synthetic modifications can influence the resulting defect geometry toward attaining desired narrow photoluminescence capacity.

DEFECT-DEPENDENT OPTICAL DIVERSITY

Pristine SWCNT Construction and Optical Properties

SWCNTs can be thought of as a pseudo one-dimensional structure of sp^2 -hybridized carbon atoms. Due to strong overlap of unhybridized p-orbitals in the carbon lattice, most chiralities of SWCNTs are semiconducting materials with a low dielectric constant.³⁶ The delocalized π -electron system results in exceptional charge-carrier diffusion and mobility of tightly bound excitons along the nanotube.³⁶ The excitons (bound states of an electron and a hole) are fundamental energy carriers, being electronic excitations of SWCNTs with about 10 nm in size, which freely move around the lattice in pristine systems.

Because there are a number of distinct ways in which a graphene sheet can be rolled to form the tubular structure, SWCNTs have a wide range of geometries. Pristine systems range in diameter from ~ 0.6 nm and larger with distinct “chiral angles” varying from 0° to 30° (Figure 1a). Due to the diversity of chemical structures of SWCNTs, their electronic and optical properties are also highly diverse. Most intense light absorption in SWCNT systems occurs between Van Hove singularities of the valence and conduction band (so-called “ E_{11} ” and “ E_{22} ” transitions, Figure 1b). Subsequent vibrational relaxation and diffusion results in an exciton that emits with a lower E_{11} energy. As a result of this confined geometry and electronic structure, emission trends with the inverse diameter of the SWCNT (neglecting the effects of chiral angle and $\text{mod}(n-m,3)$ class). The resulting range of wavelengths at which pristine SWCNTs exhibit emission features is from 800 to 1800 nm for the most commonly synthesized chiralities.³⁷ Such a diversity of optical features is one of the reasons that SWCNTs are explored for use in a wide range of applications. However, structural defects, tube ends and dark excitonic

states lying lower in energy than the optically bright transition provides a pathway for nonradiative vibronic relaxation to the ground state.³⁸ As a result, the emissive quantum yield in pristine SWCNTs is very low (generally lower than 1%). This reduces the potential for use of these materials as emitters in modern technological applications.

Electronic Structure and Emission of Functionalized SWCNTs

To alleviate this problem, covalent functionalization introduces intentional defects that cause exciton localization²⁷ resulting in the red-shifts of their energy and enhancement in quantum yields. While this increases the SWCNTs utility for optical applications owing for intensified emission, a detailed understanding of relationships between specific defect structure and resulting optical properties is needed to formulate robust synthetic and fabrication routes to achieve tunability and precise control over emission. Here we start with an overview of modeling and experimental studies that have been performed to characterize the general effect of SWCNT functionalization on their electronic and optical properties. Covalent functionalization introduces sp^3 defects into the otherwise sp^2 -hybridized lattice.^{26,30} Experimental studies clearly demonstrate that these defects act as potential wells, effectively trapping excitons,^{27,39} confining them to the functional site, and reducing the extent of the nanotube that is sampled (Figure 2).^{28,29} The resulting exciton is confined from a tube length of ~ 10 nm in the pristine system to 2–8 nm depending on the defect nature. This results in a number of practical implications for the electronic and optical properties of the functionalized system.²⁷ First, the ground-state electronic structure and energetic levels are strongly perturbed upon functionalization.¹ In pristine SWCNTs, electron density is uniformly spread across the SWCNT in both the highest-occupied molecular orbital (HOMO) and the lowest-unoccupied molecular orbital (LUMO). Both the HOMO and the LUMO are composed of two degenerate states with similar electron localization. Electron density in these degenerate states is similar in localization but located on different bonds in the hexagonal SWCNT lattice. However, functionalization breaks this degeneracy. One of the formerly degenerate HOMO states is still quite delocalized and slightly

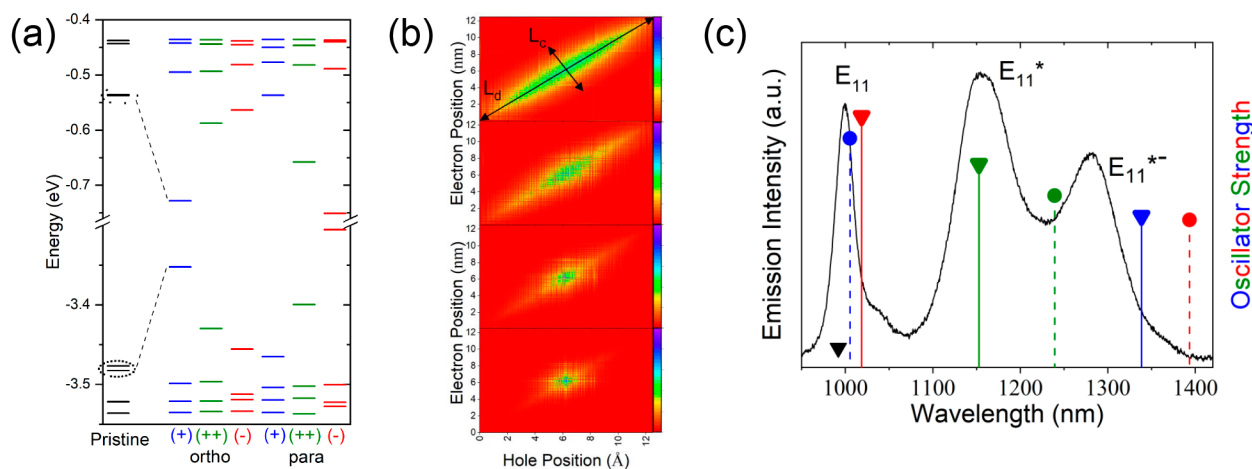


Figure 3. (a) Calculated electronic structure of pristine (black) and functionalized (colored) (6,5) SWCNTs, transition densities of pristine and ortho-functionalized species from (a), (b) transition densities for aryl-functionalized (6,5) SWCNTs, and (c) Calculated transition energies and oscillator strengths for functionalization of (6,5) SWCNTs with aryl groups, generating defects with distinct geometries. Calculated emission from ortho and para defects are presented with solid and dashed drop lines, respectively. Blue, green, and red features result from functionalization along bonds lying 27°, 87°, and −33° from the SWCNT axis, respectively. Experimental photoluminescence spectra for (6,5) SWCNTs functionalized with aryl dichloride groups (solid lines) and the computed transition energies. All data adapted with permission from ref 1. Copyright 2017 American Chemical Society.

stabilized, while the other becomes strongly localized around the defect site and strongly destabilized. The picture is reversed for the LUMO states, where the delocalized state is slightly destabilized and the strongly localized state is significantly stabilized. This results in a strong reduction of the HOMO–LUMO gap in SWCNTs upon functionalization and an accompanied modification to their optical properties (Figures 3a, 3c).

Due to this reduction of the gap, covalent functionalization dramatically alters the energetic structure of E₁₁ transitions (i.e., the bright emissive state). After breaking of degeneracy of the two HOMO states and two LUMO states, the HOMO–LUMO transition becomes the lowest energy typically bright transition¹⁷ red-shifted from the native state by ~0.1 to 0.3 eV.^{17,28,29,34,40} This enables capturing and immobilizing of mobile excitons from pristine tube segments and thus results in much stronger emission in the functionalized system with quantum yields exceeding 35%.²⁶ Moreover, the defect-associated red-shifted state provides the required conditions for a spatially localized single-photon emitter: a quantum mechanical quasi-two-level system emitting at the near-infrared spectral range (~1100–1550 nm, depending on tube chirality and functionalizing molecule). The increased quantum yield coupled with the strong red-shift in functionalized systems dramatically increases the promise of using SWCNTs as quantum emitters in a realm of practical applications.^{31,41}

Morphological, Electronic, and Spectral Diversity of Defects

While the application of SWCNTs as emitters is promoted by functionalization, this strategy also introduces additional complexity and challenges. In particular, a wide diversity of emission features are typically introduced despite the use of very pure reagents and homogeneous SWCNT samples of a single chirality.³³ Subsequently, low temperature single-tube PL spectra exhibit a range of narrow-line width features spreading across a band of energies (from 0.98 to 1.18 eV for (6,5) SWCNTs) (Figure 4a). It is apparent that such features originate from a single functionalized SWCNT since

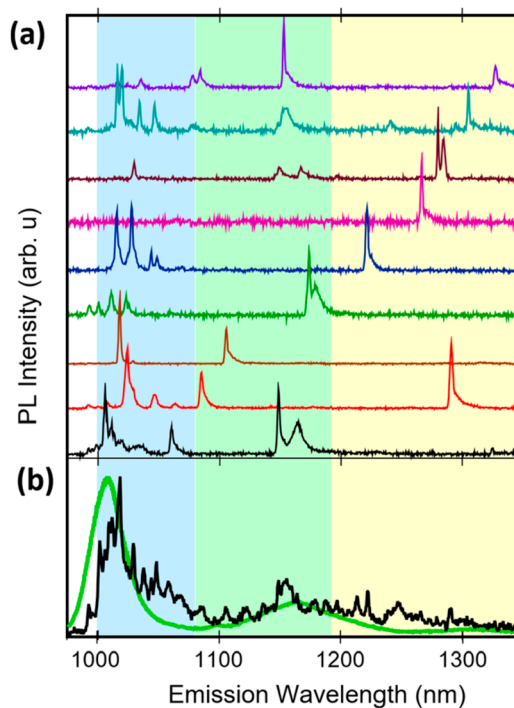


Figure 4. (a) Low-temperature PL spectra of nine individual 3,5-dichlorobenzene-functionalized (6,5) SWCNTs wrapped in PFOBPp. Emission energies of sharp defect emission peaks spread from 1050 nm (1.18 eV) to 1300 nm (0.953) eV, indicating a diversity of defect geometries. (b) Black and green lines: average low-T PL spectrum of 60 individual 3,5-dichlorobenzene-functionalized SWCNTs and ensemble, RT PL spectrum of functionalized SWCNT film, respectively. Figure reproduced with permission from ref 33. Copyright 2017 American Chemical Society.

experimental techniques break the bundles and the single defects can be clearly seen using PL imaging techniques.²⁷ Furthermore, a number of ensemble-level, solution-phase spectra demonstrates the appearance of multiple broad emission features that are separated by a wide energy range

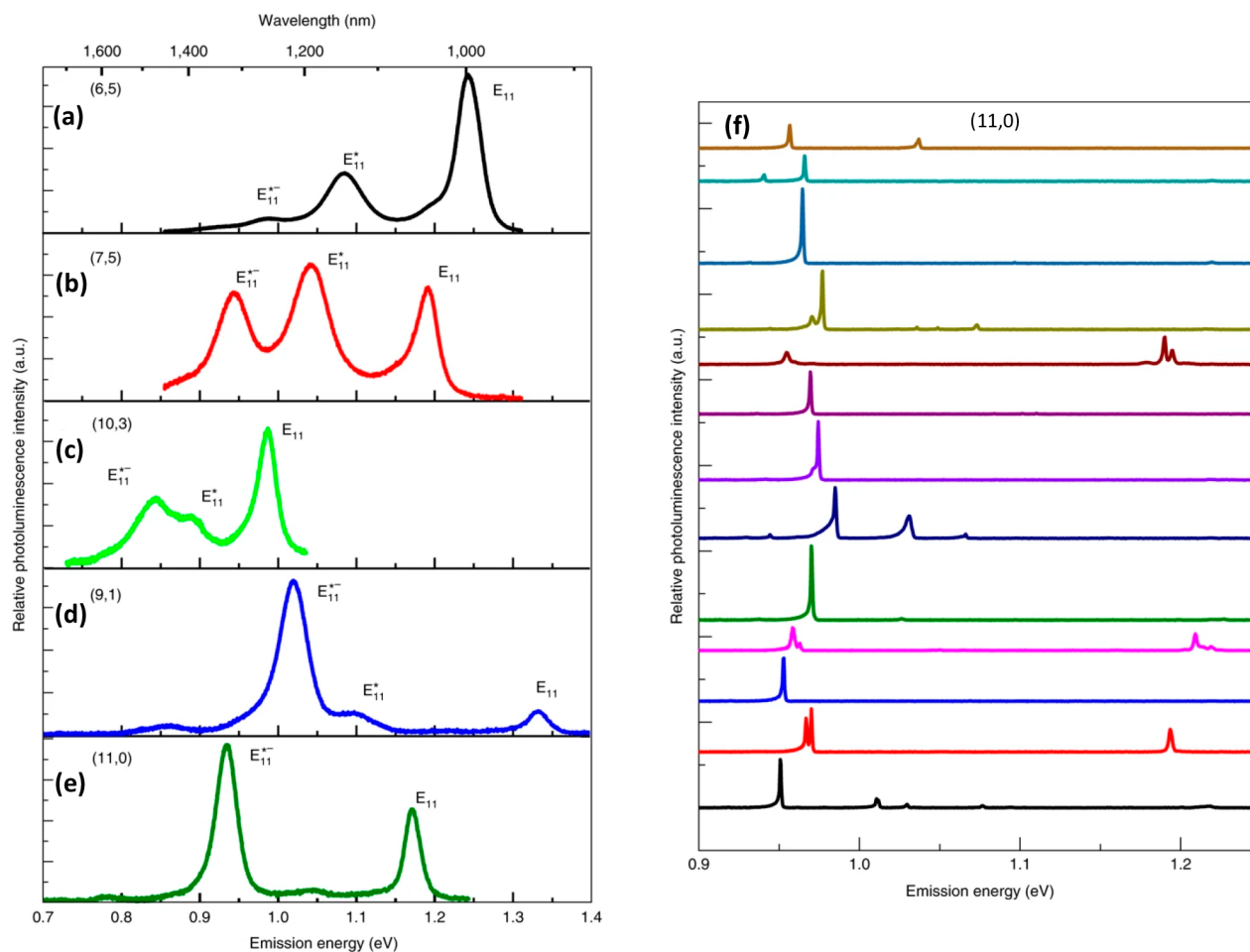


Figure 5. (a–e) Ensemble photoluminescence spectra (obtained with excitation near the E_{22} transition) of different SWCNT chiralities, (6,5), (7,5), (10,3), (9,1) and (11,0), respectively, functionalized with 4-methoxybenzene in a 1% sodium dodecyl sulfate environment. All spectra were obtained in D_2O . Two distinct defect emission bands labeled as E_{11}^+ and E_{11}^- are separated by a large energy range in the cases of (6,5), (7,5), (10,3), and (9,1) SWCNTs. Note that the difference in defect-state photoluminescence intensities relative to that of E_{11} across the chirality range reflects a difference in defect concentration. Progression in structures from nearly armchair in the case of (6,5) to the zigzag (11,0) system results in an increase in relative intensity of E_{11}^- . Spectra collapse to a single emission feature at E_{11}^- in the zigzag limit (e). (f) Low T (4 K) photoluminescence spectra of individual (11,0) SWCNTs are found within a 25 meV range of the E_{11}^- band observed in (e). Figure adapted with permission from ref 2. Copyright 2018 Nature Publishing Group.

(Figure 4b,5). This indicates that several distinct defects differing by either geometry or localized environment can be generated on the SWCNT surface.

A number of computational studies have been performed to elucidate this behavior.^{1–4,17,27,38,42,43} These studies explore the electronic and optical properties of molecular defects introduced to the surface of the SWCNT in a systematic way to give insight into the wide chemical space that is possible with these systems. Due to the extended π -electron system in the sp^2 -hybridized carbon network, binding a dopant group to a single carbon atom on the surface of the SWCNT leads to an open shell system with a reactive electron seeking another chemical bond. Thus, such a functionalization process involves the initial formation of a relatively unstable charged or radical intermediate. As a result, it will rapidly capture another species (from either the solvent, or another reactive reagent) to generate a closed-shell system. Therefore, two carbon atoms are getting functionalized. As such, the second functionalization species is generally assumed to be in close proximity to the first. It was also shown computationally that only location of functional groups at the same carbon-ring results in optically

active transitions.^{17,44} Limiting such functionalization to the same hexagonal ring, the two functionalized carbon atoms can be either adjacent to each other (the so-called “ortho” functionalization in a 1,2 fashion) or on the radially opposing site on the ring (the so-called “para” functionalization in a 1,4 fashion). Subsequently, a covalent defect in functionalized SWCNT systems is considered to consist of two functional groups in either ortho- or para-positions on the ring, with a total of six topologically distinct defect geometries due to the chiral structure of the tube.¹ All of the plausible defect geometries that result from these additions are shown in Figure 6b.

Excitons are trapped by the potential wells generated from functionalization (Figures 3b and 6a).^{27–29,45} The degree to which electrons in the frontier molecular orbitals (i.e., the depth of the potential well) are localized around the defect site is strongly dependent on the defect geometry (Figure 6a).^{17,44} Some defect geometries strongly localize electrons in the frontier molecular orbitals around the defect site, whereas for others the degree of delocalization is similar to that of the pristine tube (Figure 3b). Strong electron confinement in the

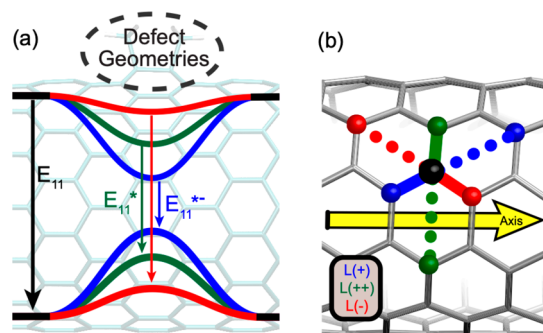


Figure 6. (a) Qualitative representation of energy levels in a functionalized SWCNT. The degree of exciton localization around the defect site, and in turn the resulting energy of emission, is dictated by the defect geometry. (b) Types of bonds present in (6,5) SWCNTs, where blue, green, and red label the bonds lying 27° , 87° , and -33° from the SWCNT axis, respectively. Functionalization restricted to the same hexagonal generates two plausible defect geometries involving 1,2 functionalization (“ortho”, solid lines) and 1,4 functionalization (“para”, dashed lines).

frontier molecular orbital underpins destabilization and stabilization of the HOMO and the LUMO, respectively, resulting in a significantly reduced energy gap (Figure 3a). A consequence of the reduction of the gap is a strong red-shift of the transitions associated with spatially defect-localized excitons (Figure 3c). This red-shift is less pronounced for defect geometries where delocalization in the frontier molecular orbitals resembles that of the pristine system. In this case, the frontier molecular orbital density, and therefore the exciton, is not localized, despite functionalization, and the electronic structure and optical energies are similar to those in pristine SWCNTs. These differences have been attributed to differences in the nodal structure of the pristine wave function, where functionalizing along node-free paths in the pristine SWCNT results in stronger electron localization.⁴

This variety in defect morphology is the source of the rich spectral diversity.^{1,33} Calculated spectral energies corrected for errors introduced by finite-size effects, approximate density functionals, and finite basis sets fall in the energy range exhibited by experiment.³⁵ Comparison of the theoretical (Figure 3c) and experimental results (Figures 4 and 5) enables the inference of which defect geometries are formed in experimental samples and targeting of specific defect geometries where specific spectral energies are desired.³³ While this rich spectral diversity potentially enables tuning of fluorescence, in order for functionalized SWCNTs to be utilized in applications, careful control over the emissive energies must be achieved particularly for an ensemble of emitters. The remainder of this Account focuses on how the SWCNT defect can be controlled toward attainment of desired spectral tuning.

■ CONTROLLING DIVERSITY OF SWCNT EMISSION

Functionalization has experimentally been shown to be effective in generating systems with a range of emissive diversity, where new red-shifted emission features labeled as E_{11}^* (at ~ 1150 nm range) and E_{11}^{*-} (at ~ 1300 nm range) for (6,5) SWCNTs, originate from different defect morphologies discussed in the previous section. With the understanding of how the formation of a distinct defect configuration generates the emissive exciton with a certain energy, three strategies for

controlling defect-state emission wavelengths are naturally suggested: (1) varying the chirality of the SWCNT,^{2,4} (2) varying the functional group itself,^{3,40,46} and (3) varying the nature of the functional group and reaction conditions to attain specific defect geometries.^{3,47} Here, we present the effects on optical diversity of using these strategies toward systematic control of the emission energy.

Nanotube Chirality

The wide range of chirality-dependent luminescence in pristine SWCNTs enables in turn diverse tunability of emission energies in functionalized samples. Similar to diameter-dependent E_{11} shifts observed in pristine SWCNTs due to one-dimensional quantum confinement, all emission features in functionalized SWCNTs also exhibit diameter-dependent energies. The red-shifts of E_{11}^* and E_{11}^{*-} with respect to the parent E_{11} peak are relatively independent of tube diameter, and the absolute red-shift energies roughly follow a trend of reverse dependence on the squared diameter: $E \sim 1/d^2$.³⁴ The extent of the exciton down the SWCNT axis is similar independent of tube diameter. These red-shifts are therefore consistent with the particle in a box as with absolute E_{11} energies. Consequently, changing the diameter of the functionalized SWCNT is an obvious strategy toward modifying their emission energies. In addition, the relative intensities of E_{11}^* and E_{11}^{*-} peaks are highly dependent on the chirality of the SWCNT.² This is rationalized by the fact that the functionalized bonds form defects with different angles with respect to the SWCNT axis, the emission energies of which highly depend on the $\text{mod}(n-m,3)$ SWCNT class. It is well-known that E_{11} energies are dependent on the mod-class.⁴ Therefore, the energies of E_{11}^* and E_{11}^{*-} are also mod/class-dependent.

Recent joint experimental and computational studies have established the role of tube chirality in controlling defect-state spectral response.² In particular, it was found that selectivity in molecular binding configuration on the nanotube surface can be achieved through aryl functionalization of “zigzag” nanotube structures (with chiral angle of zero). It was revealed that while both E_{11}^* and E_{11}^{*-} emission bands corresponding to two distinct defect geometries are clearly visible in ensemble level PL spectra of near armchair ((6,5) and (7,5) chiralities) SWCNTs in D_2O (Figure 5a, b), the E_{11}^{*-} band corresponding to a single defect geometry configuration dominates the PL spectra of the zigzag (11,0) as well as near zigzag (9,1) SWCNTs functionalized with the same functional group and dispersed in the same way (Figure 5d, e). Low temperature PL spectra of 13 individual zigzag SWCNTs (11,0 chirality) also show <25 meV inhomogeneity of emission energies (Figure 5f), standing in contrast to 0.95–1.18 eV spread of the emission peaks observed in (6,5) SWCNTs (Figure 4a). Quantum-chemical calculations confirmed that, because of the associated structural symmetry of zigzag SWCNTs, the defect states become degenerate thus limiting emission energies to a single narrow band. It was also shown that this behavior can only result from a predominant selectivity for ortho binding configurations of the aryl groups on the nanotube lattice.²

This selective functionalization can be attributed to differences in π -orbital mismatch in certain bonds of the SWCNT. Curvature in SWCNTs induces a decreased π -character of the hybridized orbitals of the carbon atoms. Due to this, the π -orbitals are not perfectly perpendicular to the pseudoplane of the tube, and each C–C bond possesses some

π -orbital mismatch,^{48–50} as illustrated in Figure 7a. Bonds near the SWCNT axis tend to have minimal π -orbital mismatch, the

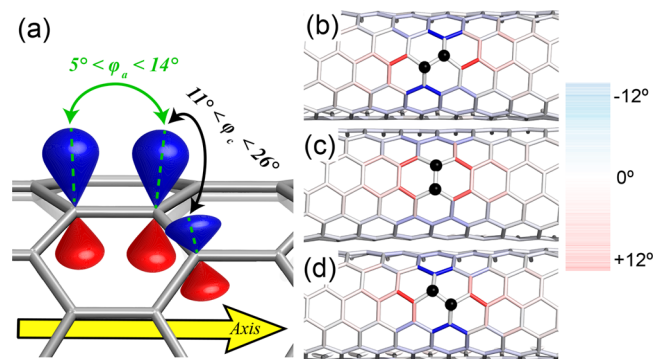


Figure 7. (a) π -Orbital mismatch for two carbon atoms lying along the axial bond (green arrow) and circumferential bond (black arrow),³⁵ and difference between the π -orbital mismatch in bonds surrounding a defect and the pristine case for a (6,5) SWCNT functionalized in the L_{30} (b), L_{90} (c), and L_{-30} (d) orientations. Figure reproduced with permission from ref 3. Copyright 2019 American Chemical Society.

magnitude of which depends on its diameter. This is also true for the bonds along the SWCNT circumference. Higher mismatch results in lower π -overlap, less electron mobility, and therefore a more destabilized system. As such, functionalizing along bonds that have stronger π -orbital mismatch (i.e., converting their carbon atoms to sp^3 hybridization and eliminating the π -orbitals) is more favorable.^{48,51} Functionalization is favored along certain bonds resulting in different defect geometries with distinct mod-dependent emission energies.⁴ Thus, using different tube chiralities is a useful strategy for controlling their emission energies via modification of binding site geometry. We will further use the phenomenon

of π -orbital mismatch to induce directing effects in the functionalization in a section below.

Inductive Effects of the Functional Group

While the presence of different defect geometries is the predominant reason for a broad emissive diversity,³ the strength of red-shift is also affected by the strength of electron inductive nature of the functional groups. Red-shifts generated in this way are typically limited to ~ 10 meV in magnitude.⁴⁰ Recent reports have used a change in the functional groups as a strategy to tune emissive energies.^{34,40} Because the degree of HOMO stabilization and LUMO destabilization (and therefore the magnitude of the red-shift) is dependent on electron density around the defect site,¹ the inductive ability of a functional group affects the resulting red-shift. In this case, an increase in the strength of the inductive ability of the group experimentally results in a stronger red-shift, whereas weaker inductive groups generate smaller red-shifts. With the goal of tuning the red-shift in mind, three strategies for modifying the inductive ability of the functional group have emerged: (1) change the functional group entirely (i.e., introduce groups with oxygen or fluorine) to increase the inductive ability and therefore the red-shift; (2) increase the number of electronegative atoms in a fixed chain (i.e., substitute hydrogen atoms in a long alkyl chain with fluorine atoms in order to systematically increase the red-shift); and (3) increase the distance between the SWCNT and electronegative atoms (i.e., increase the chain length of fluorinated alkyl groups to reduce the inductive abilities of a functional group and therefore reduce the red-shift).⁴⁰ The magnitude of red-shifts possible through these three methods varies, with changing the functional group able to tune red-shifts from ~ 130 meV to ~ 200 meV.⁴⁰

These red-shifts can be accounted for by considering the localization effect of Coulombic interactions on the electrons around the defect. Groups with strongly electronegative atoms in the close proximity to the SWCNT induce a slightly positive

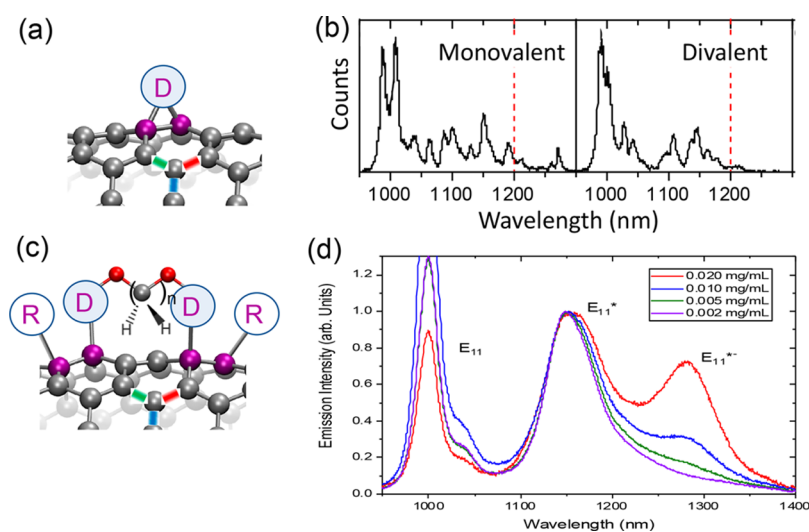


Figure 8. (a) Divalent functional group where a single atom in the functional group bonds to two atoms in the SWCNT. (b) Ensemble level spectra arising from functionalizing (6,5) SWCNT with monovalent vs divalent functional groups (where dashed red lines separate the regions of the spectra attributed to monovalent and divalent functionalization at higher and lower wavelengths respectively), (c) another type of divalent functionalization where more than one atom in the functional group functionalizes more than one atom of the SWCNT, but still with geometries limited by a fixed-length alkyl chain between the two functional group atoms, and (d) emission spectra from functionalizing (6,5) SWCNT with monovalent aryl diazonium reagents of different concentrations. Figure adapted with permission from ref 3. Copyright 2019 American Chemical Society.

charge on the carbon atom in the SWCNT that localizes electron density in the SWCNT.³ This, in turn, impacts spatial localization of the exciton near the defect, resulting in a stronger red-shift. In this way, the inductive effect is linked to electron localization around the defect, and the degree of red-shift of a functional group can be evaluated by considering that group's effect on the charge of the SWCNT atom to which the group is bound.³ In addition to a group's electron withdrawing abilities, the electron donating abilities through resonance must also be considered. For example, aryl groups generate stronger red-shifts than alkyl groups due to the stronger electron-withdrawing abilities of the sp^2 hybridized functional group carbon atoms directly bonded adjacent to the SWCNT. However, the introduction of an electronegative nitrogen atom to the aryl group results in an inductively stronger electron withdrawing group counterbalanced by resonantly stronger electron donating group. The net effect is a smaller red-shift in the species absent the electronegative nitrogen atom. Evaluating the red-shifts of functionalized SWCNT systems requires careful consideration of both inductive and resonance effects of the functional group.³ Furthermore, in all cases it is assumed that functionalizing with groups of different electronegative abilities does not drastically change the predominance of different defect geometries. This approximation appears to be valid based on the consistent relatively small red-shifts in these systems observed experimentally.⁴⁰

Modification of the Group Valency

Thus, far in this report, only functional groups that bond through a single SWCNT atom ("monovalent" functional groups) have been considered. This bonding configuration requires an auxiliary group to maintain a closed shell neutral system, the position of which determines the defect geometry. However, not all functional groups bond through a single SWCNT carbon atom. Groups bonding to two SWCNT carbon atoms are also plausible (Figure 8a). In this case, auxiliary groups are not required as a single functional group maintains a neutral closed shell system by functionalizing two adjacent SWCNT atoms. Due to constraints in the bond lengths and angles, so-called "divalent" functional groups result in the generation of specific rigid defect geometries.³⁴ Unlike the case for monovalent functional groups, specific defect geometries, where divalent functionalization occurs along the SWCNT circumference, allow the bonded SWCNT atoms to retain sp^2 hybridization as in pristine systems and are therefore stabilized. This constraint results in restricted emission energies.

Furthermore, the other defect geometries (where functionalization is close to the SWCNT axis) require bond angles with very strong angle strain. This results in an additional thermodynamic stability of one defect configuration over another. As a result, defect configurations are constrained to a single species and emissive diversity is reduced. Experimental data from a sample divalent system of this type is presented in Figure 8b. Where a single defect configuration exists, the fluorescence energies are slightly red-shifted from the monovalent counterparts. This is especially true in the case of less electron withdrawing functional groups. Such red-shifts have been attributed to the ability of the electrons to localize to the defect site due to the presence of unhybridized π -orbitals on the SWCNT carbon atoms.³ In this way, the hybridization changes from using divalent functional groups instead of monovalent species, providing a means to tune the geometries

of the defects that form. This leads to a control over large red-shifts, as well as enables tuning of the precise energies of photoluminescence.

Directing Effects for Functionalization

In addition to using thermodynamic stability to direct defects to form specific geometries (as is the case for divalent defects in the previous section), directing effects that rely on π -orbital mismatch can also be harnessed. The formation of a single defect (either monovalent or divalent) results in a perturbation of the SWCNT geometry upon functionalization. sp^2 hybridization is disrupted at the defect site by converting two tube atoms to sp^3 hybridized carbons. This perturbation to the pristine tube geometry, however, is not limited to the defect itself. The carbon-carbon bonds in the vicinity of the defect are also perturbed, affecting their π -orbital mismatch (Figure 7b-d). The exact change in π -orbital mismatch depends on the geometry of the bond. Furthermore, this effect is most pronounced very close to the defect and tapers off when the distance grows to greater than about eight bonds. As a result, the chemical reactivity in a close proximity to a defect is perturbed, with some bonds being "activated" and others being "deactivated" depending on the orientation of the first defect. In this way, an existing defect has directing effects that facilitate the production of defects in another configuration.

Performing functionalization with conditions that forces a defect to form in close proximity to another therefore directs the second defect to form with a specific defect geometry.⁴⁷ This can be accomplished in two ways: (1) use functional groups with "bridging" moieties that force two defects to form in a rigid distance from each other and (2) use different concentrations of reagents to force high or low surface coverage of defects. In the first scenario, long bridging groups allow for a large distance between two defects (such as shown in Figure 8c), and they form binding sites independent from each other. In this case, the defect geometry and emission are similar to the case for low concentrations of monovalent defects, predominantly generating the single emission feature that is generated in the monovalent case. Defects with short bridging groups, on the other hand, form in close proximity to each other. As such, two defects with different geometries appear and the emission diversity is increased.⁴⁷

Likewise, using high concentrations of reagents generates a high surface coverage of defects, thereby forcing them to appear in close proximity to each other. This convolutes directing effects on the defect geometry, and thus, two emission features are formed. However, lower concentrations of monovalent defects lack the directing effects, leading only to a singular defect geometry and thus restricting the emission to a single feature (Figure 8d). Taking advantage of these directing effects is a very powerful technique for controlling the emission energies in functionalized SWCNTs.³

CONCLUDING REMARKS

Chemical functionalization is an important strategy for increasing the quantum yield of emission of SWCNTs and expanding their functionality. However, such a route introduces a range of fluorescence features with different energies. Through computational and experimental exploration, the importance of defect geometry on emission energies has been demonstrated. The existence of a number of defect geometries makes functionalized SWCNTs more useful for applications, but only if such functionalization can be carefully

controlled to generate very precise emissive energies. A number of methods have emerged for controlling the defect geometries, aiming at narrow bands and a precise selection of desired emission energies. This mainly includes variation of the SWCNT chirality, and the functional group itself, as well as modification of the nature of the functional group and reaction conditions to select specific defect geometries. Here, we have discussed the use of these strategies and their theoretical underpinnings toward reduction of optical diversity and a systematic control of the emission energy. A combination of these methods provides a powerful toolbox to experimentally control the emission energies in functionalized SWCNTs. Where large red-shifts are desired, defect geometry can be controlled by functionalizing with divalent groups where some geometries will become less thermodynamically stable. Stronger or weaker red-shifts can be accomplished through functionalization with different chiralities with both different chiral angles and $\text{mod}(n-m,3)$ classes. Finally, red-shifts can be finely tuned by integrating groups with different electron inducing abilities. This detailed understanding enables the continued design of functionalized SWCNTs toward realization of room-temperature robust single photon near-IR quantum emitters with robust high efficiencies.

AUTHOR INFORMATION

Corresponding Authors

Stephen K. Doorn – *Center for Integrated Nanotechnologies, Materials Physics and Applications Division, Los Alamos National Laboratory, Los Alamos, New Mexico 87545, United States*; orcid.org/0000-0002-9535-2062; Email: skdoorn@lanl.gov

Sergei Tretiak – *Center for Nonlinear Studies, Center for Integrated Nanotechnologies, Materials Physics and Applications Division, and Theoretical Division, Los Alamos National Laboratory, Los Alamos, New Mexico 87545, United States*; orcid.org/0000-0001-5547-3647; Email: serg@lanl.gov

Authors

Brendan J. Gifford – *Center for Nonlinear Studies, Center for Integrated Nanotechnologies, Materials Physics and Applications Division, and Theoretical Division, Los Alamos National Laboratory, Los Alamos, New Mexico 87545, United States*; orcid.org/0000-0002-4116-711X

Svetlana Kilina – *Department of Chemistry and Biochemistry, North Dakota State University, Fargo, North Dakota 58108, United States*; orcid.org/0000-0003-1350-2790

Han Htoon – *Center for Integrated Nanotechnologies, Materials Physics and Applications Division, Los Alamos National Laboratory, Los Alamos, New Mexico 87545, United States*; orcid.org/0000-0003-3696-2896

Complete contact information is available at:
<https://pubs.acs.org/10.1021/acs.accounts.0c00210>

Notes

The authors declare no competing financial interest.

Biographies

Brendan J. Gifford is a Scientist for the Physics and Chemistry of Materials group in the Theory Division at Los Alamos National Laboratory (LANL). He was born in Cameron, Wisconsin in 1986 where he was raised. He received his B.Sc. degree in Chemistry from University of Wisconsin—Stevens Point in 2011 and his Ph.D. in

Chemistry from North Dakota State University in 2017 working for Svetlana Kilina. He began working at LANL as a student in 2016 and began a postdoc in 2018 working under Sergei Tretiak. He was converted to Scientist in 2019 where his current research interests include the electronic structure of functionalized nanomaterials, machine learning of molecular properties, and opacities of hot dense matter.

Svetlana Kilina obtained her Ph.D. in Chemistry at the University of Washington in 2007. In 2008–2010, she worked as the Director's Postdoctoral Fellowship at Los Alamos National Laboratory. Since Fall 2010, she holds an appointment as a faculty member at the Chemistry and Biochemistry Department, North Dakota State University and currently is James A. Meier Associate Professor. She is the recipient of an Early Career Research Award from the Department of Energy (2012) and a Sloan Foundations Award (2014). Her research is on the frontiers of computational chemistry and nanoscale materials science with a particular focus on inorganic–organic interfaces and photoexcited dynamics.

Han Htoon is a scientist at the Center for Integrated Nanotechnologies, Los Alamos National Laboratory. He was born in April, 1967 in Yangon, Myanmar. He received B.Sc. in Physics at Yangon University (1991), M.S. in Physics at Western Illinois University (1996), and Ph.D. in Physics at University of Texas at Austin with C. K. Shih (2001). He joined Los Alamos National Laboratory as a Director Postdoctoral Fellow under Victor I. Klimov. He became a staff scientist in 2005. Since his Ph.D. studies, his research efforts have focused on the development of novel single nanostructure optical spectroscopy techniques and study of the fundamental and quantum optical properties of a variety of optical nanomaterials including quantum dots, quantum wires, SWCNTs, and two-dimensional materials. For his recent efforts in revealing potential of covalent color centers of SWCNTs in quantum light generation applications, he was selected as the fellow of American Physical Society (2017) and also awarded Los Alamos National Laboratory Fellow Research Prize (2019).

Stephen K. Doorn, born in 1963 in Wisconsin, received his B.S. degree in Chemistry from the University of Wisconsin, and earned his M.S. (1986) and Ph.D. (1990) degrees in Physical Chemistry at Northwestern University. Stephen began his career at Los Alamos National Laboratory (LANL) as a Director's Postdoctoral Fellow (1990). He continued on as a Staff Scientist, performing spectroscopic materials characterization. Most recently, he has served nearly 10 years as the co-thrust leader for the Nanophotonics and Optical Nanomaterials research thrust in the Center for Integrated Nanomaterials at LANL. Recently retired from LANL, Stephen maintains a guest scientist status with the laboratory. Research interests have included development of surface enhanced Raman active nanoparticles for bioanalytical applications and resonance Raman and fluorescence spectroscopy, as well as covalent and noncovalent surface chemistry, of single wall carbon nanotubes. Recent efforts include research on fundamental photophysics, chemistry, and quantum light emission behavior arising from sp^3 defects of carbon nanotubes. Stephen is the recipient of the Los Alamos National Laboratory's Fellows Prize for Research and is an APS Fellow and a LANL Fellow.

Sergei Tretiak is a Staff Scientist at Los Alamos National Laboratory. He received his M.Sc. degree from Moscow Institute of Physics and Technology (Russia) in 1994 and his Ph.D. degree in 1998 from the University of Rochester. Since 2006, he has been a member of the DOE funded Center for Integrated Nanotechnologies (CINT). He also serves as an Adjunct Professor at the University of California,

Santa Barbara (2015–present) and at Skolkovo Institute of Science and Technology, Moscow, Russia (2013–present). His research interests include development of modern computational methods for molecular optical properties, nonlinear optical response of organic chromophores, adiabatic and nonadiabatic molecular dynamics of excited states, optical response of confined excitons in conjugated polymers, carbon nanotubes, semiconductor nanoparticles, halide perovskites, molecular aggregates as well as data science complementing conventional quantum chemistry applications.

ACKNOWLEDGMENTS

This work was conducted in part at the Center for Nonlinear Studies and the Center for Integrated Nanotechnologies (CINT), U.S. Department of Energy, Office of Basic Energy Sciences (DOE BES) user facility. It is also supported in part by Los Alamos National Laboratory (LANL) Directed Research and Development Funds (LDRD). This research used resources provided by the LANL Institutional Computing (IC) Program. S.K. acknowledges the DOE EPSCoR: Building EPSCoR-State/National Laboratory Partnerships Grant #0000253864 for support of the productive collaborations between LANL and North Dakota State University (NDSU). H.H., S.K.D., and B.J.G. acknowledge the support from DOE BES FWP LANLBES22, Deterministic Placement and Integration of Quantum Defects. Finally, the authors acknowledge Braden Weight (North Dakota State University, CINT) for preparation of Figure 6b as well as Avishek Saha, Xiaowei He, and Younghee Kim for figure preparation. LANL is operated by Triad National Security, LLC, for the National Nuclear Security Administration of the U.S. Department of Energy (Contract No. 89233218NCA000001).

REFERENCES

- Gifford, B. J.; Kilina, S.; Htoon, H.; Doorn, S. K.; Tretiak, S. Exciton Localization and Optical Emission in Aryl-Functionalized Carbon Nanotubes. *J. Phys. Chem. C* **2018**, *122* (3), 1828–1838.
- Saha, A.; Gifford, B. J.; He, X.; Ao, G.; Zheng, M.; Kataura, H.; Htoon, H.; Kilina, S.; Tretiak, S.; Doorn, S. K. Narrow-Band Single-Photon Emission through Selective Aryl Functionalization of Zigzag Carbon Nanotubes. *Nat. Chem.* **2018**, *10* (11), 1089.
- Gifford, B. J.; He, X.; Kim, M.; Kwon, H.; Saha, A.; Sifain, A. E.; Wang, Y.; Htoon, H.; Kilina, S.; Doorn, S. K.; Tretiak, S. Optical Effects of Divalent Functionalization of Carbon Nanotubes. *Chem. Mater.* **2019**, *31* (17), 6950–6961.
- Gifford, B. J.; Saha, A.; Weight, B. M.; He, X.; Ao, G.; Zheng, M.; Htoon, H.; Kilina, S.; Doorn, S. K.; Tretiak, S. Mod($n-m,3$) Dependence of Defect-State Emission Bands in Aryl-Functionalized Carbon Nanotubes. *Nano Lett.* **2019**, *19* (12), 8503–8509.
- Iijima, S. Helical Microtubules of Graphitic Carbon. *Nature* **1991**, *354* (6348), 56–58.
- Saito, R. *Physical Properties of Carbon Nanotubes*; Saito, R., Dresselhaus, M. S., Eds.; Imperial College Press, 1998.
- Dass, D.; Prasher, R.; Vaid, R. Analytical Study Of Unit Cell And Molecular Structures Of Single Walled Carbon Nanotubes. *Int. J. Comput. Eng. Res.* **2012**, *2* (6), 1447–1457.
- Ando, T. Theory of Electronic States and Transport in Carbon Nanotubes. *J. Phys. Soc. Jpn.* **2005**, *74* (3), 777–817.
- O'connell, M. J.; Bachilo, S. M.; Huffman, C. B.; Moore, V. C.; Strano, M. S.; Haroz, E. H.; Rialon, K. L.; Boul, P. J.; Noon, W. H.; Kittrell, C. Band Gap Fluorescence from Individual Single-Walled Carbon Nanotubes. *Science* **2002**, *297*, 593–596.
- Kataura, H.; Kumazawa, Y.; Maniwa, Y.; Umez, I.; Suzuki, S.; Ohtsuka, Y.; Achiba, Y. Optical Properties of Single-Wall Carbon Nanotubes. *Synth. Met.* **1999**, *103* (1), 2555–2558.
- He, X.; Hartmann, N. F.; Ma, X.; Kim, Y.; Ihly, R.; Blackburn, J. L.; Gao, W.; Kono, J.; Yomogida, Y.; Hirano, A.; Tanaka, T.; Kataura, H.; Htoon, H.; Doorn, S. K. Tunable Room-Temperature Single-Photon Emission at Telecom Wavelengths from Sp^3 Defects in Carbon Nanotubes. *Nat. Photonics* **2017**, *11* (9), 577–582.
- Wolf, S. A.; Awschalom, D. D.; Buhrman, R. A.; Daughton, J. M.; von Molnár, S.; Roukes, M. L.; Chtchelkanova, A. Y.; Treger, D. M. Spintronics: A Spin-Based Electronics Vision for the Future. *Science* **2001**, *294* (5546), 1488–1495.
- Ravindran, S.; Chaudhary, S.; Colburn, B.; Ozkan, M.; Ozkan, C. S. Covalent Coupling of Quantum Dots to Multiwalled Carbon Nanotubes for Electronic Device Applications. *Nano Lett.* **2003**, *3*, 447–453.
- Mason, N.; Biercuk, M. J.; Marcus, C. M. Local Gate Control of a Carbon Nanotube Double Quantum Dot. *Science* **2004**, *303*, 655–658.
- Li, J.; Papadopoulos, C.; Xu, J. M.; Moskovits, M. Highly-Ordered Carbon Nanotube Arrays for Electronics Applications. *Appl. Phys. Lett.* **1999**, *75*, 367.
- Hertel, T.; Himmelein, S.; Ackermann, T.; Stich, D.; Crochet, J. Diffusion Limited Photoluminescence Quantum Yields in 1-D Semiconductors: Single-Wall Carbon Nanotubes. *ACS Nano* **2010**, *4* (12), 7161–7168.
- Kilina, S.; Ramirez, J.; Tretiak, S. Brightening of the Lowest Exciton in Carbon Nanotubes via Chemical Functionalization. *Nano Lett.* **2012**, *12*, 2306–2312.
- Zhang, H.; Wu, B.; Hu, W.; Liu, Y. Separation and/or Selective Enrichment of Single-Walled Carbon Nanotubes Based on Their Electronic Properties. *Chem. Soc. Rev.* **2011**, *40* (3), 1324–1336.
- Reich, S.; Thomsen, C.; Ordejon, P. Electronic Band Structure of Isolated and Bundled Carbon Nanotubes. *Phys. Rev. B: Condens. Matter Mater. Phys.* **2002**, *65*, 155411.
- Tasis, D.; Tagmatarchis, N.; Bianco, A.; Prato, M. Chemistry of Carbon Nanotubes. *Chem. Rev.* **2006**, *106*, 1105–1136.
- Li, H.; Gordeev, G.; Garrity, O.; Peyyety, N. A.; Selvasundaram, P. B.; Dehm, S.; Krupke, R.; Cambre, S.; Wenseleers, W.; Reich, S.; Zheng, M.; Fagan, J. A.; Flavel, B. S. Separation of Specific Single-Enantiomer Single-Wall Carbon Nanotubes in the Large-Diameter Regime. *ACS Nano* **2020**, *14* (1), 948–963.
- Yang, F.; Wang, M.; Zhang, D.; Yang, J.; Zheng, M.; Li, Y. Chirality Pure Carbon Nanotubes: Growth, Sorting, and Characterization. *Chem. Rev.* **2020**, *120* (5), 2693–2758.
- Dai, H.; Rinzler, A. G.; Nikolaev, P.; Thess, A.; Colbert, D. T.; Smalley, R. E. Single-Wall Nanotubes Produced by Metal-Catalyzed Disproportionation of Carbon Monoxide. *Chem. Phys. Lett.* **1996**, *260* (3), 471–475.
- Kitiyanan, B.; Alvarez, W. E.; Harwell, J. H.; Resasco, D. E. Controlled Production of Single-Wall Carbon Nanotubes by Catalytic Decomposition of CO on Bimetallic Co–Mo Catalysts. *Chem. Phys. Lett.* **2000**, *317* (3), 497–503.
- Miyauchi, Y.; Iwamura, M.; Mouri, S.; Kawazoe, T.; Ohtsu, M.; Matsuda, K. Brightening of Excitons in Carbon Nanotubes on Dimensionality Modification. *Nat. Photonics* **2013**, *7* (9), 715–719.
- Piao, Y.; Meany, B.; Powell, L. R.; Valley, N.; Kwon, H.; Schatz, G. C.; Wang, Y. Brightening of Carbon Nanotube Photoluminescence through the Incorporation of Sp^3 Defects. *Nat. Chem.* **2013**, *5* (10), 840–845.
- Hartmann, N. F.; Yalcin, S. E.; Adamska, L.; Hároz, E. H.; Ma, X.; Tretiak, S.; Htoon, H.; Doorn, S. K. Photoluminescence Imaging of Solitary Dopant Sites in Covalently Doped Single-Wall Carbon Nanotubes. *Nanoscale* **2015**, *7* (48), 20521–20530.
- Adamska, L.; Nayyar, I.; Chen, H.; Swan, A. K.; Oldani, N.; Fernandez-Alberti, S.; Golder, M. R.; Jasti, R.; Doorn, S. K.; Tretiak, S. Self-Trapping of Excitons, Violation of Condon Approximation, and Efficient Fluorescence in Conjugated Cycloparaphenylenes. *Nano Lett.* **2014**, *14* (11), 6539–6546.
- Kim, M.; Adamska, L.; Hartmann, N. F.; Kwon, H.; Liu, J.; Velizhanin, K. A.; Piao, Y.; Powell, L. R.; Meany, B.; Doorn, S. K.; Tretiak, S.; Wang, Y. Fluorescent Carbon Nanotube Defects Manifest

Substantial Vibrational Reorganization. *J. Phys. Chem. C* **2016**, *120* (20), 11268–11276.

(30) Ghosh, S.; Bachilo, S. M.; Simonette, R. A.; Beckingham, K. M.; Weisman, R. B. Oxygen Doping Modifies Near-Infrared Band Gaps in Fluorescent Single-Walled Carbon Nanotubes. *Science* **2010**, *330* (6011), 1656–1659.

(31) He, X.; Htoon, H.; Doorn, S. K.; Pernice, W. H. P.; Pyatkov, F.; Krupke, R.; Jeantet, A.; Chassagneux, Y.; Voisin, C. Carbon Nanotubes as Emerging Quantum-Light Sources. *Nat. Mater.* **2018**, *17* (8), 663.

(32) Luo, Y.; He, X.; Kim, Y.; Blackburn, J. L.; Doorn, S. K.; Htoon, H.; Strauf, S. Carbon Nanotube Color Centers in Plasmonic Nanocavities: A Path to Photon Indistinguishability at Telecom Bands. *Nano Lett.* **2019**, *19* (12), 9037–9044.

(33) He, X.; Gifford, B. J.; Hartmann, N. F.; Ihly, R.; Ma, X.; Kilina, S. V.; Luo, Y.; Shayan, K.; Strauf, S.; Blackburn, J. L.; Tretiak, S.; Doorn, S. K.; Htoon, H. Low-Temperature Single Carbon Nanotube Spectroscopy of Sp³ Quantum Defects. *ACS Nano* **2017**, *11* (11), 10785–10796.

(34) Kim, M.; Wu, X.; Ao, G.; He, X.; Kwon, H.; Hartmann, N. F.; Zheng, M.; Doorn, S. K.; Wang, Y. Mapping Structure-Property Relationships of Organic Color Centers. *Chem.* **2018**, *4* (9), 2180–2191.

(35) Gifford, B. J.; Sifain, A. E.; Htoon, H.; Doorn, S. K.; Kilina, S.; Tretiak, S. Correction Scheme for Comparison of Computed and Experimental Optical Transition Energies in Functionalized Single-Walled Carbon Nanotubes. *J. Phys. Chem. Lett.* **2018**, *9* (10), 2460–2468.

(36) Saito, R.; Dresselhaus, G.; Dresselhaus, M. S. *Physical Properties of Carbon Nanotubes*; Imperial College Press: London, 1998.

(37) Bachilo, S. M. Structure-Assigned Optical Spectra of Single-Walled Carbon Nanotubes. *Science* **2002**, *298* (5602), 2361–2366.

(38) Kilina, S.; Badaeva, E.; Piryatinski, A.; Tretiak, S.; Saxena, A.; Bishop, A. R. Bright and Dark Excitons in Semiconductor Carbon Nanotubes: Insights from Electronic Structure Calculations. *Phys. Chem. Chem. Phys.* **2009**, *11*, 4113–4123.

(39) Danné, N.; Kim, M.; Godin, A. G.; Kwon, H.; Gao, Z.; Wu, X.; Hartmann, N. F.; Doorn, S. K.; Lounis, B.; Wang, Y.; Cognet, L. Ultrashort Carbon Nanotubes That Fluoresce Brightly in the Near-Infrared. *ACS Nano* **2018**, *12* (6), 6059–6065.

(40) Kwon, H.; Furmanchuk, A.; Kim, M.; Meany, B.; Guo, Y.; Schatz, G. C.; Wang, Y. Molecularly Tunable Fluorescent Quantum Defects. *J. Am. Chem. Soc.* **2016**, *138* (21), 6878–6885.

(41) Högele, A.; Galland, C.; Winger, M.; Imamoglu, A. Photon Antibunching in the Photoluminescence Spectra of a Single Carbon Nanotube. *Phys. Rev. Lett.* **2008**, *100* (21), 217401.

(42) Gifford, B. J. Strategic Functionalization of Single Walled Carbon Nanotubes to Manipulate Their Electronic and Optical Properties. Ph.D. Thesis, 2017.

(43) Gifford, B. J. Functionalized Carbon Nanotube Excited States and Optical Properties. In *Computational Photocatalysis: Modeling of Photophysics and Photochemistry at Interfaces*; ACS Symposium Series; American Chemical Society, 2019; Vol. 1331, pp 181–207.

(44) Ramirez, J.; Mayo, M. L.; Kilina, S.; Tretiak, S. Electronic Structure and Optical Spectra of Semiconducting Carbon Nanotubes Functionalized by Diazonium Salts. *Chem. Phys.* **2013**, *413*, 89–101.

(45) Adamska, L.; Nazin, G. V.; Doorn, S. K.; Tretiak, S. Self-Trapping of Charge Carriers in Semiconducting Carbon Nanotubes: Structural Analysis. *J. Phys. Chem. Lett.* **2015**, *6* (19), 3873–3879.

(46) Shiraki, T.; Uchimura, S.; Shiraishi, T.; Onitsuka, H.; Nakashima, N. Near Infrared Photoluminescence Modulation by Defect Site Design Using Aryl Isomers in Locally Functionalized Single-Walled Carbon Nanotubes. *Chem. Commun.* **2017**, *53* (93), 12544–12547.

(47) Shiraki, T.; Shiraishi, T.; Juhász, G.; Nakashima, N. Emergence of New Red-Shifted Carbon Nanotube Photoluminescence Based on Proximal Doped-Site Design. *Sci. Rep.* **2016**, *6*, 28393.

(48) Haddon, R. C. π -Electrons in Three Dimensions. *Acc. Chem. Res.* **1988**, *21* (6), 243–249.

(49) Haddon, R. C. Hybridization and the Orientation and Alignment of π -Orbitals in Nonplanar Conjugated Organic Molecules: π -Orbital Axis Vector Analysis (POAV2). *J. Am. Chem. Soc.* **1986**, *108* (11), 2837–2842.

(50) Haddon, R. C. GVB and POAV Analysis of Rehybridization and π -Orbital Misalignment in Non-Planar Conjugated Systems. *Chem. Phys. Lett.* **1986**, *125* (3), 231–234.

(51) Haddon, R. C. Chemistry of the Fullerenes: The Manifestation of Strain in a Class of Continuous Aromatic Molecules. *Science* **1993**, *261* (5128), 1545–1550.